Available online at www.sciencedirect.com
SCIENCE DIRECT®
Journal of Organometallic Chemistry 690 (2005) 3229–3236
Journal of Organometallic Chemistry
www.elsevier.com/locate/jorganchem

Reactivity of the dinuclear platina-β-diketone $[Pt_2\{(COMe)_2H\}_2(\mu\text{-}Cl)_2]$ towards chelating ligands – Bridge cleavage versus formation of acetyl(chloro)platinum(II) complexes

Tushar Gosavi, Christoph Wagner, Harry Schmidt, Dirk Steinborn *

Institut für Anorganische Chemie, Martin-Luther-Universität Halle-Wittenberg, Kurt-Mothes-Straße 2, D-06120 Halle, Germany

Received 10 January 2005; revised 4 March 2005; accepted 4 March 2005
Available online 23 May 2005

Abstract

The dinuclear platina-β-diketone $[Pt_2\{(COMe)_2H\}_2(\mu\text{-}Cl)_2]$ (**1**) was found to react with 2-$(ROCH_2)C_5H_4N$ (R = Me, **2a**; H, **2b**) yielding a cationic mononuclear platina-β-diketone $[Pt\{(COMe)_2H\}\{2\text{-}(MeOCH_2)C_5H_4N\}]Cl$ (**3**) and an acetyl(chloro)platinum(II) complex $[Pt(COMe)Cl\{2\text{-}(HOCH_2)C_5H_4N\}]$ (**4**), respectively. The reaction of **1** with 8-(methylthio)quinoline (**5**) resulted in the formation of $[Pt(COMe)Cl\{8\text{-}(MeS)C_9H_6N\}]$ (**6**). The identities of all complexes were established by microanalysis, ^1H, and ^{13}C NMR spectroscopy. Single-crystal X-ray diffraction analysis showed **6** to be square–planar platinum(II) complex with N and C atoms as well as Cl and S atoms in mutually *trans* positions (configuration index: *SP*-4-2). In accordance with this, quantum chemical calculations on the DFT level of theory revealed a higher stability of complex **6** having a *SP*-4-2 configuration vs. the analogous complex in *SP*-4-3 configuration. The distinctly different reactivity of **1** with **2a** on the one hand and with **2b** and **5** on the other is discussed in terms of the HSAB concept and a deprotonation/reprotonation reaction.

Keywords: Platinum; Platina-β-diketones; Acylplatinum complexes; *N*,*O* ligands; *N*,*S* ligands

1. Introduction

Formal replacement of the central methine group in the enolic form of a 1,3-diketone by a metal unit L_xM results in the formation of a metalla-β-diketone. Such complexes (Type **I**, Scheme 1) were firstly prepared by C.M. Lukehart [1]. All these complexes are electronically saturated (18 ve; ve – valence electrons) and kinetically inert. In contrast, we found that the reaction of hexachloroplatinic acid with alkynylsilanes in butanol results in the formation of dinuclear platina-β-diketones (Type **II**, Scheme 1) being electronically unsaturated (16 ve) kinetically labile complexes [2]. Due to that, reactivity of Type **I** and Type **II** metalla-β-diketones proved to be fundamentally different.

Typically, the platina-β-diketone **1** (Type **II**, R = Me) afforded to react with chelating L⌒L donors according to the reaction sequence shown in Scheme 2. Soft/soft and hard/soft donors (P⌒P, S⌒S, N⌒S) tend to react yielding stable acetyl(chloro)platinum(II) complexes (**C**) [3]. On the other hand, hard/hard donors (N⌒N) of dipyridyl and phenanthroline type gave rise to the formation of stable acetyl(hydrido)platinum(IV) complexes (**B**) that may undergo reductive elimination reaction (**B** → **C**) only at temperatures above 140 °C in the solid state [4]. Reactions with diazadiene ligands RN=CR′=CR′=NR were found to proceed in dependence on the substituents R/R′ either with the formation of type **C** complexes or with the formation of complexes **D** having enamine–amide type ligands [5]. Furthermore,

* Corresponding author. Tel.: +49 345 55 25620; fax: +49 345 55 27028.
E-mail address: dirk.steinborn@chemie.uni-halle.de (D. Steinborn).

0022-328X/$ - see front matter © 2005 Elsevier B.V. All rights reserved.
doi:10.1016/j.jorganchem.2005.03.053

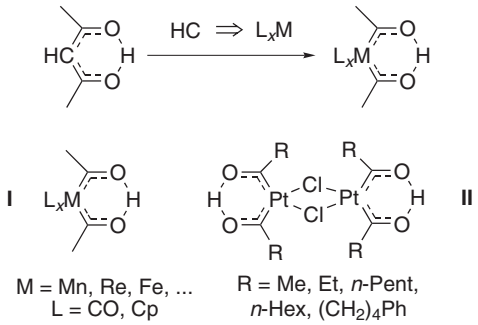

Scheme 1.

hard/hard donors 2-(RHN)C_5H_4N (R = H, Me) reacted to give cyclic aminocarbene complexes **E**, most likely because the formation of **B/C** type complexes would result in complexes having energetically unfavored four-membered rings [6].

Here we report reactions of the platina-β-diketone **1** with 2-(methoxymethyl)- and 2-(hydroxymethyl)pyridine as well as with 8-(methylthio)quinoline being hard/hard N⌒O donors and a hard/soft N⌒S donor, respectively.

2. Results and discussion

2.1. Synthesis

Reaction of the platina-β-diketone **1** with the chelating *N,O* ligands 2-(methoxymethyl)pyridine (**2a**) and 2-(hydroxymethyl)pyridine (**2b**) in tetrahydrofuran (thf) at −40 °C and then at room temperature was found to proceed according to Scheme 3. In the case of **2a**, the cationic mononuclear platina-β-diketone complex **3** was obtained in 37% yield. On the other hand, the reaction of **2b** resulted in the formation of the acetyl(chloro)platinum(II) complex **4** in 46% yield. Both the complexes were isolated as slightly air-sensitive off-white substances. Complex **3** is freely soluble in chloroform, dichloromethane and acetone while **4** is only moderately soluble in these solvents. Solutions of **3** in dichloromethane at room temperature undergo partial decomposition within one day. Identities of complexes **3** and **4** were proved by microanalysis as well as by ^1H and ^{13}C NMR measurements.

As with **2b**, the platina-β-diketone **1** was found to react with the chelating 8-(methylthio)quinoline **5** (Scheme 3). Reaction in thf at −40 °C and then at room temperature resulted in the formation of the acetyl(chloro)platinum(II) complex **6** which was isolated as a pale yellow microcrystalline substance in 42% yield. Complex **6** is slightly air-sensitive and freely soluble in ethanol, chloroform and acetone but insoluble in diethyl ether. Identity of **6** was confirmed by microanalysis, NMR measurements (^1H, ^{13}C) and by single-crystal X-ray diffraction analysis.

2.2. Spectroscopic characterization

In the NMR spectra of the mononuclear platina-β-diketone complex **3** two sets of signals for the $(COMe)_2H$ unit show the unsymmetrical coordination at platinum. Although **3** is a cationic complex, its NMR spectroscopic

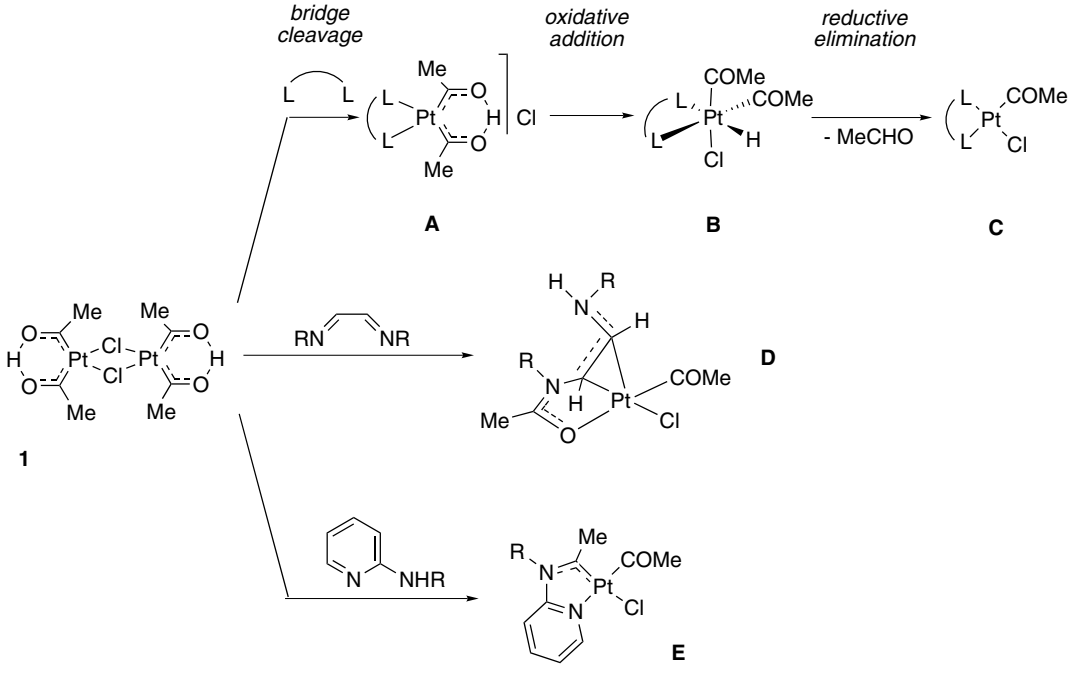

Scheme 2.

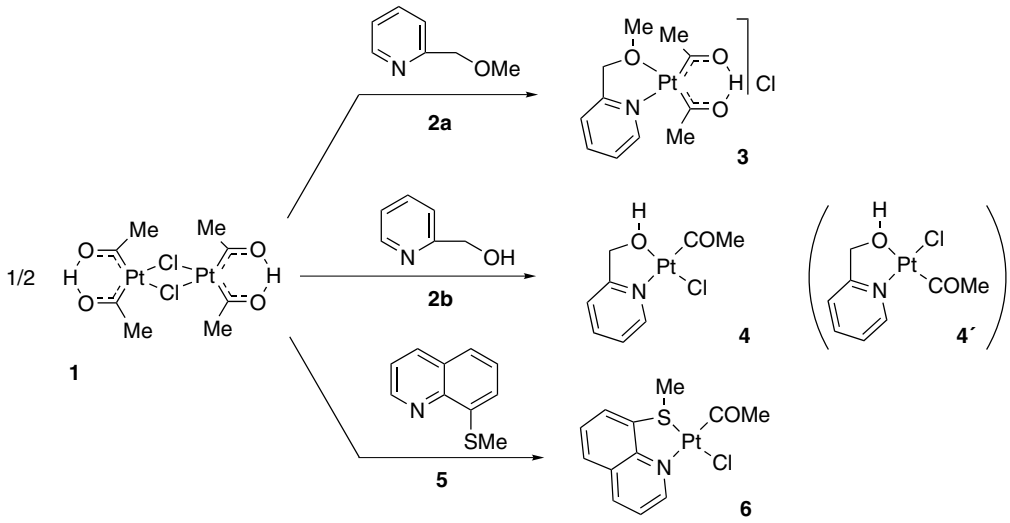

Scheme 3.

parameters are very close to those of neutral mononuclear platina-β-diketone complexes [Pt{(COMe)$_2$H}Cl(L)] (L = py, **7a**; quin, **7b**) [3a]: *C*O, δ_C 233.6/243.5 (**3**), 236.9/245.0 (**7a**), 234.2/243.8 (**7b**), $^1J_{Pt,C}$ = 1350.9/1289.3 Hz (**3**), 1361/1295 Hz (**7a**), 1353/1290 Hz (**7b**). Coordination of the lateral methoxy group (δ_H 3.51, δ_C 73.9) is clearly shown by the platinum–carbon coupling $^2J_{Pt,C}$ = 38.6 Hz. Furthermore, formation of the five-membered ring Pt–N–C–CH_2–O gives rise to a broad AB pattern for the methylene protons at 4.88/4.98 ppm with the coupling $^2J_{H,H}$ = 14.1 Hz.

Due to restricted solubility of the acetyl(chloro)platinum complex **4** with the 2-(hydroxymethyl)pyridine ligand, the resonance of the carbonyl carbon atom was not found. Comparison of chemical shifts of the methyl group of the acetyl ligand (δ_H 2.37, δ_C 42.1) with those in complex **6** (see below) indicate that in complex **4** the pyridine and acetyl ligand are in mutual *trans* position (configuration index: *SP*-4-2) although the other isomer (**4′**, Scheme 3) having the configuration index *SP*-4-3 cannot strictly be ruled out.

NMR parameters for the acetyl(chloro)platinum(II) complex **6** with the 8-(methylthio)quinoline ligand are close to those of analogous complexes with N⁀S chelate ligands such as [Pt(COMe)Cl{2-(RSCH$_2$)C$_5$H$_4$N}] (**8**, R = Et, Ph, *t*-Bu) [3b]: *C*OCH$_3$: δ_C 209.4 in **6** vs. 207.3–209.7 ppm in **8**, $^1J_{Pt,C}$ = 890.9 vs. 867–890 Hz; CO*CH*$_3$: δ_C 43.4 in **6** vs. 43.2–53.6 ppm in **8**, δ_H 2.52 vs. 2.35–2.43 ppm, $^2J_{Pt,C}$ = 105.1 vs. 110 Hz (R = Et). Assignments of quinoline protons and carbon atoms given in the experimental are based on H,H COSY, C,H COSY and NOE experiments.

2.3. Structural investigation

Crystals of the 8-(methylthio)quinoline complex **6** suitable for single-crystal X-ray diffraction analysis were grown from $CDCl_3$ solutions at room temperature. In the unit cell, separated molecules of **6** were found without unusual intermolecular interactions between them (shortest contact between non-hydrogen atoms: C5···N′ 3.292(7) Å). The molecular structure of **6** is shown in Fig. 1, selected bond lengths and angles are given Table 1. The platinum atom is slightly distorted square–planar coordinated by the *N*,*S* chelate ligand, an acetyl ligand *trans* to N and a chloro ligand *trans* to S (configuration index: *SP*-4-2). The five-membered Pt–N–C–C–S ring has an envelope conformation on S; the methyl substituent is axially oriented. The two six-membered rings of the quinoline ligand are not strictly coplanar; they include an angle of 3.3(2)°. The acetyl ligand includes with the complex plane an angle of 52.4(5)°.

The platinum–carbon and –chlorine bonds in **6** are of the same length as those in [Pt(COMe)Cl{2-(PhSCH$_2$)C$_5$H$_4$N-κ*N*,*S*}] (**8**) having the same configuration as **6** (Cl *trans* to S and C *trans* to N): **6**/**8** Pt–C11

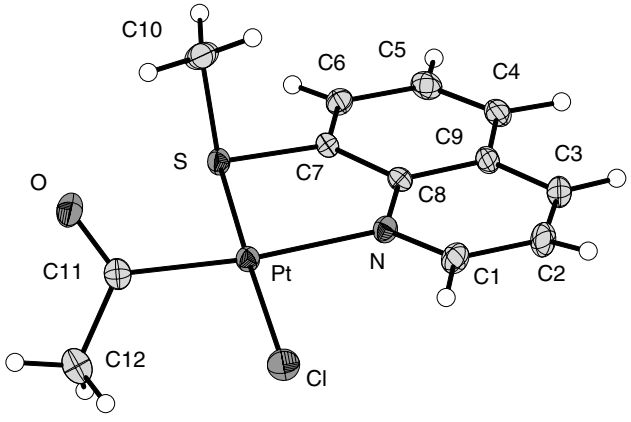

Fig. 1. Molecular structure of [Pt(COMe)Cl{8-(MeS)C$_9$H$_6$N-κ*N*,*S*}] (**6**) in the solid state. Displacement ellipsoids are drawn at 30% probability.

Table 1
Selected bond lengths (in Å) and angles (°) for the complex [Pt(COMe)Cl{8-(MeS)C_9H_6N-κ*N*,*S*}]

	6	6c	9c
Pt–Cl	2.325(l)	2.364	2.358
Pt–N	2.170(3)	2.272	2.111
Pt–S	2.240(l)	2.325	2.505
Pt–C11	1.998(5)	2.004	2.013
S–C7	1.784(4)	1.803	1.792
S–C10	1.823(5)	1.842	1.839
O–C11	1.220(6)	1.220	1.220
Cl–Pt–S	176.68(4)	175.0	89.0
Cl–Pt–C11	92.8(l)	92.9	91.6
S–Pt–C11	89.4(l)	92.0	176.2
Cl–Pt–N	93.3(l)	92.8	170.6
S–Pt–N	84.7(l)	82.3	82.8
N–Pt–C11	173.7(2)	174.2	96.6
Pt–N–C8	115.6(3)	116.9	119.6
Pt–S–C7	100.4(2)	101.3	96.1
Pt–S–C10	105.4(2)	105.1	104.9

Complex **6**: solid-state structure, experimental values (*SP*-4-2 isomer); complex **6c**: gas-phase structure, calculated values (*SP*-4-2 isomer); complex **9c**: gas-phase structure, calculated values (*SP*-4-3 isomer).

1.998(5)/1.997(6) Å, Pt–Cl 2.325(1)/2.320(2) Å. On the other hand, on the basis of the 3σ criterion the platinum–nitrogen and –sulfur bonds are shorter in **6** than in **8** (Pt–N 2.170(3)/2.190(5) Å, Pt–S 2.240(1)/2.257(2) Å).

2.4. Computational results

To get insight into factors that may influence the structure of complex **6** we performed quantum chemical calculations on the DFT level of theory. The calculated structure **6c** is shown in Fig. 2a. It is close to the experimentally found structure **6** as the comparison of selected geometric parameters in Table 1 reveals. In the calculated structure **6c** the quinoline ligand is planar (greatest deviation from the mean plane 0.011 Å for C6). To understand the position of the acetyl ligand with respect to the complex plane, a scan of the potential energy surface for the O–C11–Pt–S angle was performed (Fig. 3). The calculated angle is close to that in the solid state structure (−45.8 vs. −52.7°) corresponding to an energy difference of 0.3 kcal/mol only. From Fig. 3, it is obvious that the energetically most disfavored structure is about 12 kcal/mol higher in energy than the equilibrium structure and has a dihedral angle O–C11–Pt–S of about 180°. This may be due electrostatic repulsion between the chloro ligand and the C=O group (distance Cl···O ≈ 3.0 Å; Mulliken charges in electrons: q(Cl) = −0.29, q(O) = −0.34) and steric interactions between the two methyl groups (distance C···C ≈ 3.2 Å).

A marked feature of the structure of complex **6/6c** is the position of the methyl substituent on the sulfur atom being almost perpendicular to the complex plane, both in the experimentally found and in the calculated structure.

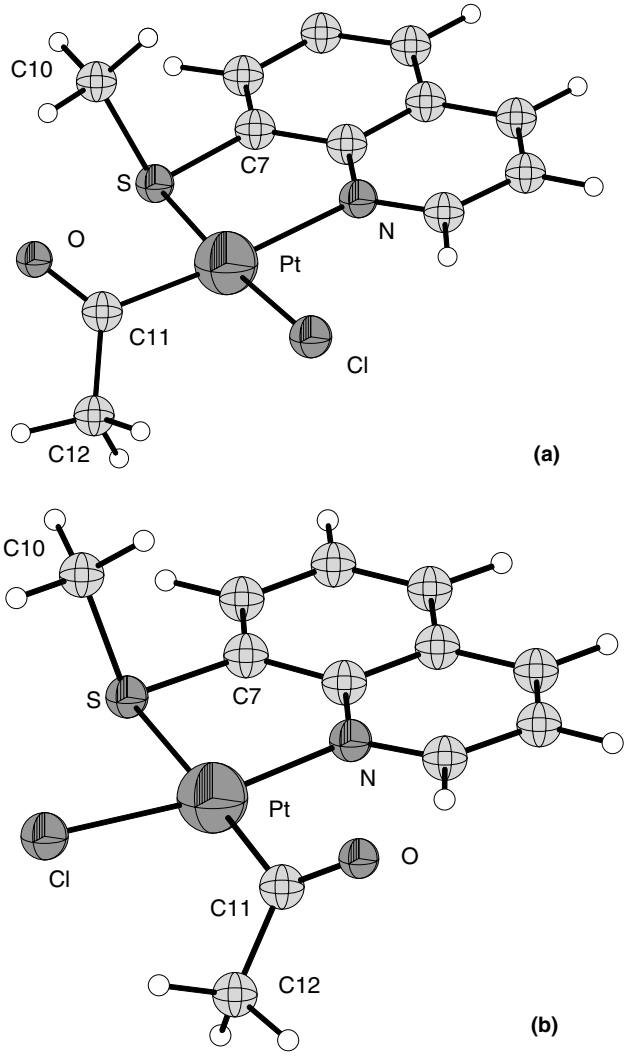

Fig. 2. Calculated structures in the gas phase of the two isomeric complexes [Pt(COMe)Cl{8-(MeS)C_9H_6N-κ*N*,*S*}] along with their numbering schemes: (a) complex **6c**, *SP*-4-2 isomer; (b) complex **9c**, *SP*-4-3 isomer.

The scan of the potential energy surface for the C11–Pt–S–C10 coordinate (being a measure for the position of the methyl group $C10H_3$ in relation to the complex plane) is shown in Fig. 4. The equilibrium structures **6c** and **6c′** are equivalent; they are related by an inversion operation. The dihedral angle in the equilibrium structure **6c** was calculated to be 73.5° (**6c′**: −73.5°) and in the experimentally found structure (**6**) 83.7° corresponding to an energy difference of 0.3 kcal/mol only. Thus, this difference between calculated and experimental structure may be caused – at least in part – by packing effects in the crystal. The highest energy ($\Delta E \approx 11$ kcal/mol) along the C11–Pt–S–C10 coordinate was found for a complex having the methyl group in the complex plane. As shown in Fig. 4 to force the dihedral angle C11–Pt–S–C10 to be 0° gives rise to severe distortions of the coordination geometry. No equilibrium structure corresponding to a complex with an "equatorial" position of the S–CH_3

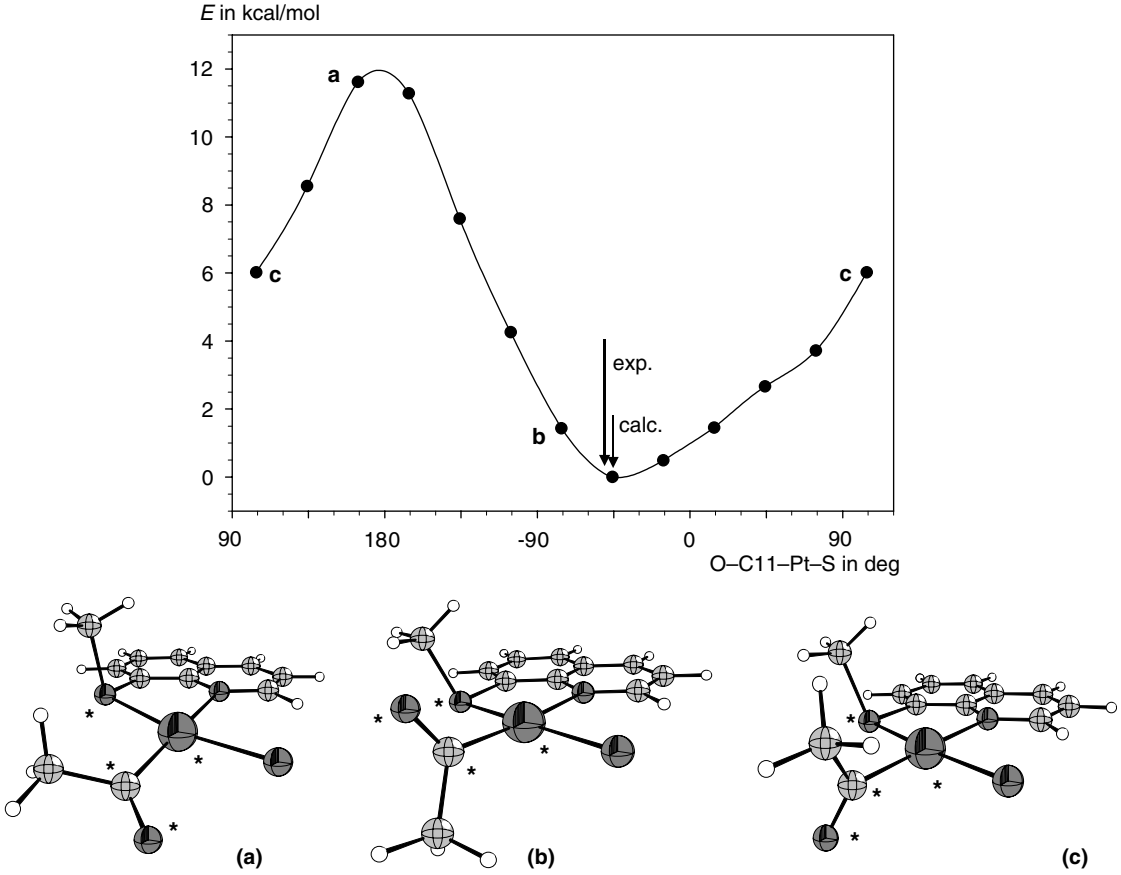

Fig. 3. Conformational energy diagram of the O–C11–Pt–S coordinate in [Pt(COMe)Cl{8-(MeS)C_9H_6N-κ*N*,*S*}] (**6c**). Torsion angles of the calculated equilibrium structure **6c** and the experimentally found structure (**6**) are marked by arrows. Molecular structures for selected torsion angles O–C11–Pt–S (+164.2°, **a**; −75.8°, **b**; +104.2°, **c**) are given on the bottom (atoms defining the torsion angle are marked by asterisks).

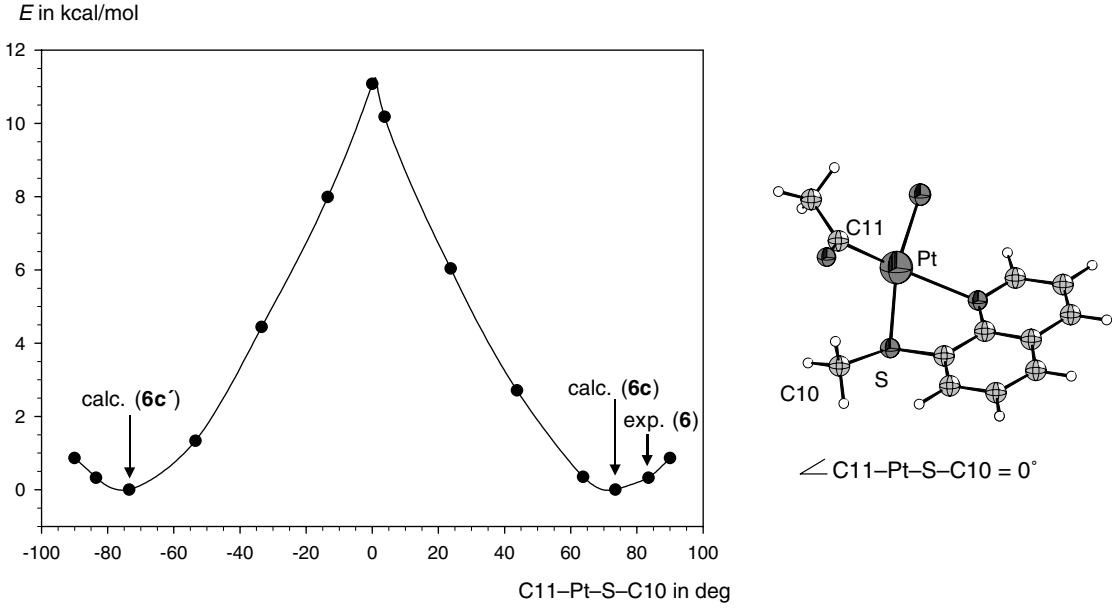

Fig. 4. Conformational energy diagram of the C11–Pt–S–C10 coordinate in [Pt(COMe)Cl{8-(MeS)C_9H_6N-κ*N*,*S*}] (**6c**). Torsion angles of the calculated equilibrium structures (**6c**/**6c**′) and the experimentally found structure (**6**) are marked by arrows. On the right hand side the structure with the highest energy (C11–Pt–S–C10 0°) is shown.

group could be localized on the potential surface. However, according to the NBO analysis of complex **6c** the direction of the lone electron pair on sulfur has to be characterized by a dihedral angle C11–Pt–S–lp (lp – lone electron pair) of about −40°.

The complex **6** and **6c**, respectively, has the configuration index *SP*-4-2. That is, the C and N atoms as well as the S and Cl atoms are in mutual *trans* positions. To make clear whether the other possible diastereomer (configuration index: *SP*-4-3) is more or less stable, its structure and energy have been also calculated on the same level of theory. The equilibrium structure **9c** is shown in Fig. 2b, selected bond lengths and angles are given in Table 1. The strong *trans* influence of the acetyl ligand (compared with the chloro ligand) is reflected in a longer Pt–S bond in **9c** (*Δ* 0.180 Å) and in a longer Pt–N bond in **6c** (*Δ* 0.161 Å). Complex **6c** was found to be more stable than **9c** by 3.70 kcal/mol and by 3.68 kcal/mol when the zero-point vibrational energies were taken into consideration.

2.5. Conclusions

The reaction of 8-(methylthio)quinoline with the dinuclear platina-β-diketone **1** yielding a type **C** complex (Scheme 2) is fully in accord with the reactivity of other N⁀S donor ligands having pyridine and thioether type donor sites [3b]. Most likely, the reaction proceeds via an (unseen) type **B** intermediate, a bis(acetyl)hydridoplatinum(IV) complex. Its instability may be due to the general observation that organoplatinum(IV) complexes are better stabilized by hard than by soft donor co-ligands [7]. Furthermore, the quantum chemical calculations on the stability of the diastereomers **6c** and **9c** indicate that the experimentally formed complex **6** (Scheme 3) is the thermodynamically more stable diastereomer.

The completely different reactivity of 2-(methoxymethyl)pyridine **2a** and 2-(hydroxymethyl)pyridine **2b** (Scheme 3) having analogous donor sites deserve explanation. With a (monodentate) pyridine type donor the dinuclear platina-β-diketone **1** was found to react with bridge cleavage forming type **A** complexes [Pt{(COMe)$_2$H}Cl(L)] (**7**, L = py, quin) [3a], cf. Scheme 2. The same reaction proceeds with **2a** yielding **3**, but instead of Cl the lateral methoxy group is coordinated. Assuming that with **2b** the reaction starts in the same way, the further reaction **A** → **B** → **C** (Scheme 2) may be induced by a deprotonation of the lateral hydroxy group on a small extent. This may be why the deprotonated ligand has a much stronger anionic donor site exerting a much higher *trans* influence and effect, respectively [8]. The final step forming **4** can be supposed to be the reprotonation of the anionic N⁀O$^-$ ligand.

To summarize, these studies have not only shown the synthesis and characterization of the first stable cationic platina-β-diketone complex **3** but also how precisely the reactivity of platina-β-diketones can be tuned by co-ligands.

3. Experimental

3.1. General

All reactions were performed under an Ar atmosphere using standard Schlenk techniques. Solvents were dried (Et_2O and thf over Na–benzophenone) and distilled prior to use. ^{1}H and ^{13}C NMR spectra were recorded on Varian Gemini 200, VXR 400, and Unity 500 NMR spectrometers. Chemical shifts are relative to C*H*Cl$_3$ (δ 7.24) and *C*DCl$_3$ (δ 77.0) as internal references. Assignments of NMR signals were partly revealed by COSY experiments (^{1}H,^{1}H; ^{1}H,^{13}C). Microanalyses were performed by the University of Halle microanalysis laboratory using CHNS-932 (LECO) and Vario EL (elementar Analysensysteme) elemental analyzers. The complex [Pt$_2${(COMe)$_2$H}$_2$(μ-Cl)$_2$] (**1**) [2a], 2-(methoxymethyl)pyridine (**2a**) [9], and 8-(methylthio)quinoline (**5**) [10] were prepared according to published methods. 2-(Hydroxymethyl)pyridine (**2b**) was commercially (ACROS) available.

3.2. Syntheses

3.2.1. Preparation of complexes [Pt{(COMe)$_2$H}{2-(MeOCH$_2$)C$_5$H$_4$N}] Cl (3) and [Pt(COMe)Cl{2-(HOCH$_2$)C$_5$H$_4$N}] (4)

To a suspension of [Pt$_2${(COMe)$_2$H}$_2$(μ-Cl)$_2$] (**1**) (50 mg, 0.08 mmol) in thf (4 ml) the compound 2-(ROCH$_2$)C$_5$H$_4$N (R = Me, **2a**; H, **2b**; 0.16 mmol) was added at −40 °C. The pale yellow suspension immediately changed the color to colorless solution. The reaction mixture was warmed up to room temperature over 15–20 min upon stirring. Seventy percent of the total volume of thf was removed in vacuo. Then diethyl ether was added dropwise till the formation of a precipitate was observed. The mixture was kept at −40 °C overnight yielding off-white powdery precipitate that was filtered off, washed with diethyl ether (5 ml) and dried briefly in vacuo.

Complex ***3***. Yield: 26 mg (37%). Anal. Calc. for C$_{11}$H$_{16}$ClNO$_3$Pt (440.78): C, 29.97; H, 3.66; N, 3.18. Found: C, 30.29; H, 4.18; N, 3.10%. ^{1}H NMR (400 MHz, CD_2Cl_2): δ 1.74/2.64 (s + d/s + d, ^3J(Pt,H) = 19.34/18.26 Hz, ≈2.6H/3H, 2 × COC*H*$_3$; reduced intensity of one signal for unknown reason), 3.51 (s, 3H, CH$_2$OC*H*$_3$), 4.88 (H$_A$)/4.98 (H$_B$) (AB pattern, ^2J(H$_A$,H$_B$) = 14.1 Hz, 2H, C*H*$_A$*H*$_B$OMe), 7.45 (t, ^3J(H5,H4) = ^3J(H5,H6) = 6.45 Hz, lH, 5-C*H*$_{py}$), 7.76 (d, ^3J(H3,H4) = 7.62 Hz, lH, 3-C*H*$_{py}$), 7.95 (t, ^3J(H4,H3) = ^3J(H4,H5) = 7.65 Hz, lH, 4-C*H*$_{py}$), 8.67 (d, ^3J(H6,H5) = 5.37 Hz, lH, 6-C*H*$_{py}$), ca. 17.6 (br,

0.5H, O*H*O). ^{13}C NMR (126 MHz, $CDCl_3$): δ 39.2/40.4 (s + d/s + d, ^2J(Pt,C) = 165.5/140.6 Hz, 2 × CO*C*H$_3$), 59.3 (s, *C*H$_2$OCH$_3$), 73.9 (s + d, ^2J(Pt,C) = 38.6 Hz, CH$_2$O*C*H$_3$), 124.1/124.6 (s/s, 3/5-*C*$_{py}$), 139.0 (s, 4-*C*$_{py}$), 150.3 (s, 6-*C*$_{py}$), 159.5 (s, 2-*C*$_{py}$), 233.6/243.5 (s + d/s + d, ^1J(Pt,C) = 1350.9/1289.3 Hz, 2 × *C*OCH$_3$). Overnight measurement at room temperature to identify Pt–C couplings resulted in partly decomposition due to restricted stability of complex.

Complex ***4***. Yield: 28 mg (46%). M.p. 110–112 °C (dec.). Anal. Calc. for $C_8H_{10}ClNO_2Pt$ (382.70): C, 25.11; H, 2.63; N, 3.66. Found: C, 26.34; H, 2.73; N, 3.94%. ^{1}H NMR (400 MHz, CD_2Cl_2): δ 2.37 (s, 3H, COC*H*$_3$), 5.12 (s, 2H, C*H*$_2$OH), 7.19 (t, ^3J(H5,H4) = ^3J(H5,H6) = 6.33 Hz, 1H, 5-C*H*$_{py}$), 7.27 (d, ^3J(H3,H4) = 7.06 Hz, 1H, 3-C*H*$_{py}$), 7.87 (td, ^3J(H4,H3) = ^3J(H4,H5) = 7.68 Hz, ^4J(H4,H6) = 1.25 Hz, 1H, 4-C*H*$_{py}$), 8.19 (d + d (br), ^3J(H6,H5) = 5.60 Hz, ^3J(Pt,H) = 56.44 Hz, 1H, 6-C*H*$_{py}$), 9.84 (br, 1H, CH$_2$O*H*). ^{13}C NMR (101 MHz, $CDCl_3$): δ 42.1 (s, CO*C*H$_3$), 67.9 (s, *C*H$_2$OH), 120.8/124.9 (3/5-*C*$_{py}$), 137.7 (4-*C*$_{py}$), 150.2 (6-*C*$_{py}$), 162.1 (2-*C*$_{py}$). Due to the restricted solubility and stability the resonance for the carbonyl carbon atom was not found.

3.2.2. Preparation of [Pt(COMe)Cl{8-(MeS)C$_9$H$_6$N}] (*6*)

To a suspension of [Pt$_2${(COMe)$_2$H}$_2$(μ-Cl)$_2$] (**1**) (50 mg, 0.08 mmol) in thf (4 ml) 8-(methylthio)quinoline (**5**; 28 mg, 0.16 mmol) was added at −40 °C. The yellow suspension immediately changed the color to pale yellow colored solution. The reaction mixture was warmed up to room temperature over 15–20 min upon stirring. Seventy percent of the total volume of thf was removed in vacuo. Then diethyl ether (10–15 ml) was added resulting in formation of an oily mass. The mixture was kept at −40 °C for three days and then the precipitate was filtered off, washed with diethyl ether (5 ml) and dried briefly in vacuo.

Yield: 30 mg (42%). Anal. Calc. for $C_{12}H_{12}ClNOPtS$ (448.83): C, 32.11; H, 2.69; N, 3.12. Found: C, 31.85; H, 2.67; N, 3.12%. ^{1}H NMR (400 MHz, $CDCl_3$): δ 2.52 (s, 3H, COC*H*$_3$), 3.02 (s + d, ^3J(Pt,H) = 78.81 Hz, 3H, SC*H*$_3$), 7.68–7.75 (m, 2H, 3-C*H*$_{quin}$ + 6-C*H*$_{quin}$), 7.96–8.09 (m, 1H, 5-C*H*$_{quin}$), 8.11 (d, ^3J(H7,H6) = 1.25 Hz, 1H, 7-C*H*$_{quin}$), 8.45 (dd, ^3J(H4,H3) = 8.30 Hz, ^4J(H4,H5) = ^4J(H4,H2) = 1.66 Hz, 1H, 4-C*H*$_{quin}$), 9.80 (dd, ^3J(H2,H3) = 4.88 Hz, ^4J(H2,H4) = 1.56 Hz, 1H, 2-C*H*$_{quin}$). ^{13}C NMR (101 MHz, $CDCl_3$): δ 29.8 (s + d, ^2J(Pt,C) = 29.6 Hz, SC*H*$_3$), 43.4 (s + d, ^2J(Pt,C) = 105.1 Hz, CO*C*H$_3$), 123.1 (s, 3-*C*$_{quin}$), 128.2 (s, 6-*C*$_{quin}$), 130.3 (s, 4a-*C*$_{quin}$), 130.8 (s, 5-*C*$_{quin}$), 132.2/146.8 (s + d/s + d, ^{2+3}J(Pt,C) = 30.0/54.0 Hz 8/8a-*C*$_{quin}$), 134.8 (s + d, ^3J(Pt,C) = 53.2 Hz, 7-*C*$_{quin}$), 139.2 (s, 4-*C*$_{quin}$), 151.4 (s, 2-*C*$_{quin}$), 209.4 (s + d, ^1J(Pt,C) = 890.9 Hz, *C*OCH$_3$).

3.3. X-ray structure determination

Crystals of **6** suitable for X-ray diffraction measurements were obtained from $CDCl_3$ solutions. Intensity data were collected on a STOE IPDS diffractometer at 220(2) K using graphite monochromatized Mo K$_\alpha$, radiation (λ = 0.71073 Å). A summary of the crystallographic data, the data collection parameters, and the refinement parameters is given in Table 2. Absorption correction was applied numerically (T_{min}/T_{max} 0.025/0.377). The structure was solved by direct methods with SHELXS-97 and refined using full-matrix least-squares routines against F^2 with SHELXL-97 [11]. Non-hydrogen atoms were refined with anisotropic displacement parameters. All H atoms were found in the difference Fourier map and refined isotropically with fixed U_{iso} = 0.08 Å^2 according to the riding model.

3.4. Computational details

All DFT calculations were carried out by the GAUSSIAN 98 program package [12] using the hybrid functional B3LYP [13]. For the main group atoms the basis 6-31G* was employed. The valence shell of platinum has been approximated by a split valence basis set too, for its core orbitals an effective core potential in combination with consideration of relativistic effects has been used [14]. All systems have been fully optimized without any symmetry restrictions. The resulting geometries were characterized as equilibrium structures by the analysis of the force constants of normal vibrations. The natural bond orbital (NBO) analysis was used as implemented in GAUSSIAN 98 [15].

Table 2
Crystallographic and data collection parameters for complex **6**

Empirical formula	$C_{12}H_{12}ClNOPtS$
M_r	448.83
Crystal size (mm)	0.36 × 0.36 × 0.09
Crystal system	Monoclinic
Space group	*C*2/*c*
Unit cell dimensions	
a (Å)	16.239(3)
b (Å)	10.904(2)
c (Å)	15.228(3)
β (°)	107.20(2)
V (Å)	2575.7(8)
Z	8
D_{calc}/g cm^{-1}	2.315
μ(Mo Kα)/mm^{-1}	11.246
F(000)	1680
θ range (°)	2.28–24.99
Refln. collected	8464
Refln. observed [$I > 2\sigma(I)$]	2131
Refln. independent	2258 (R_{int} = 0.0811)
Data/restraints/parameters	2258/0/190
Goodness-of-fit on F^2	1.113
R_1, wR_2 [$I > 2\sigma(I)$]	0.0275, 0.0635
R_I, wR_2 (all data)	0.0295, 0.0648
Largest diff. peak and hole (e Å^{-3})	1.427 (near Pt atom) and −1.170

Acknowledgments

We gratefully acknowledge support by the Deutsche Forschungsgemeinschaft. We also thank the company Merck (Darmstadt) for gifts of chemicals.

Appendix A. Supplementary data

Crystallographic data (excluding structure factors) for the structure reported in this paper have been deposited at the Cambridge Crystallographic Data Center (CCDC) as Supplementary Publication No. CCDC-252330 (**6**). Copies of the data can be obtained free of charge on application to the CCDC, 12 Union Road, Cambridge, CB2 1EZ, UK (fax (internat.): +44 1223 336033; e-mail: deposit@ccdc.cam.ac.uk). Tables of Cartesian coordinates of atom positions calculated for equilibrium structures **6c**, **6c′** and **9c** as well as energies of **6c** in dependence on dihedral angles O–C11–Pt–S and C11–Pt–S–C10. Supplementary data associated with this article can be found, in the online version at doi:10.1016/j.jorganchem.2005.03.053.

References

[1] (a) C.M. Lukehart, Acc. Chem. Res. 14 (1981) 109;
(b) C.A Lukehart, Adv. Organomet. Chem. 25 (1986) 45.
[2] (a) D. Steinborn, M. Gerisch, K. Merzweiler, K. Schenzel, K. Pelz, H. Bögel, J. Magull, Organometallics 15 (1996) 2454;
(b) D. Steinborn, M. Gerisch, T. Hoffmann, C. Bruhn, G. Israel, F.W. Müller, J. Organomet. Chem. 598 (2000) 286.
[3] (a) M. Gerisch, F.W. Heinemann, C. Bruhn, J. Scholz, D. Steinborn, Organometallics 18 (1999) 564;
(b) T. Gosavi, E. Rusanov, H. Schmidt, D. Steinborn, Inorg. Chim. Acta 357 (2004) 1781.
[4] D. Steinborn, A. Vyater, C. Bruhn, M. Gerisch, H. Schmidt, J. Organomet. Chem. 597 (2000) 10.
[5] A. Vyater, C. Wagner, K. Merzweiler, D. Steinborn, Organometallics 21 (2002) 4369.
[6] T. Gosavi, C. Wagner, K. Merzweiler, H. Schmidt, D. Steinborn, Organometallics 24 (2005) 533.
[7] (a) L.M. Rendina, R.J. Puddephatt, Chem. Rev. 97 (1997) 1735;
(b) D, M. Crumpton-Bregel, K.I. Goldberg, J. Am. Chem. Soc. 125 (2003) 9442.
[8] T.G. Appleton, H.C. Cark, L.E. Manzer, Coord. Chem. Rev. 10 (1973) 335.
[9] L. Canovese, L. Cattalini, G. Marangoni, M.L. Tobe, J. Chem. Soc., Dalton Trans. (1985) 731.
[10] A. Albert, G.B. Barlin, J. Chem. Soc. (1959) 2384.
[11] G.M. Sheldrick, SHELXS-97, SHELXL-97, Programs for Crystal Structure Determination, University of Göttingen, Göttingen, 1990/1997.
[12] M.J. Frisch, G.W. Trucks, H.B. Schlegel, G.E. Scuseria, M.A. Robb, J.R. Cheeseman, V.G. Zakrzewski, J.A. Montgomery Jr., R.E. Stratmann, J.C. Burant, S. Dapprich, J.M. Millam, A.D. Daniels, K.N. Kudin, M.C. Strain, O. Farkas, J. Tomasi, V. Barone, M. Cossi, R. Cammi, B. Mennucci, C. Pomelli, C. Adamo, S. Clifford, J. Ochterski, G.A. Petersson, P.Y. Ayala, Q. Cui, K. Morokuma, D.K. Malick, A.D. Rabuck, K. Raghavachari, J.B. Foresman, J. Cioslowski, J.V. Ortiz, B.B. Stefanov, G. Liu, A. Liashenko, P. Piskorz, I. Komaromi, R. Gomperts, R.L. Martin, D.J. Fox, T. Keith, M.A. Al-Laham, C.Y. Peng, A. Nanayakkara, C. Gonzalez, M. Challacombe, P.M.W. Gill, B. Johnson, W. Chen, M.W. Wong, J.L. Andres, C. Gonzalez, M. Head-Gordon, E.S. Replogle, J.A. Pople, GAUSSIAN 98, Revision A.3, Gaussian, Inc., Pittsburgh, PA, 1998.
[13] (a) A.D. Becke, Phys. Rev. A 38 (1988) 3098;
(b) A.D. Becke, J. Chem. Phys. 98 (1993) 5648;
(c) C. Lee, W. Yang, R.G. Parr, Phys. Rev. B 37 (1988) 785;
(d) P.J. Stephens, F.J. Devlin, C.F. Chabalowski, M.J. Frisch, J. Phys. Chem. 98 (1994) 11623.
[14] D. Andrae, U. Häußermann, M. Dolg, H. Stoll, H. Preuß, Theor. Chim. Acta 77 (1990) 123.
[15] (a) E.D. Glendening, A.E. Reed, J.E. Carpenter, F. Weinhold, NBO Version 3.1;
(b) A.E. Reed, R.B. Weinstock, F. Weinhold, J. Chem. Phys. 83 (1985) 735.